PCCP

Accepted Manuscript

ROYAL SOCIETY OF CHEMISTRY

www.rsc.org/pccp

Physical Chemistry Chemical Physics
CREATED USING THE RSC LaTeX PCCP ARTICLE TEMPLATE – SEE www.rsc.org/electronicfiles FOR DETAILS
ARTICLE TYPE www. rsc.org/xxxxxx | XXXXXXXX

Effects of kinetic and transport phenomena on thermal explosion and oscillatory behaviour in a spherical reactor with mixed convection

Filipa Gonçalves de Azevedo,[a‡] John F. Griffiths,[b] and Silvana S. S. Cardoso*[a]

Received Xth XXXXXXXXXX 20XX, Accepted Xth XXXXXXXXX 20XX
First published on the web Xth XXXXXXXXXX 200X
DOI: 10.1039/b000000x

Thermal explosions are often influenced by the complex interaction between transport and reaction phenomena. In particular, reactant consumption can promote safer, non-explosive operation conditions of combustion systems. However, in liquids or gases, the presence of forced convection can affect the behaviour of a system, instigating oscillations in the temperature, reactant concentration and velocity fields. This work describes the effect of reactant consumption on a simple, one-step, exothermic reaction occurring in a spherical reactor with both forced and natural convection, by means of numerical simulations. Regime diagrams characterised by ratios of timescales for each transport and reaction phenomena are presented and the explosion boundary is represented for several forced convection and reaction consumption intensities. Special attention is given to the oscillatory behaviour observed for moderate forced convection and oscillatory regions are represented on the regime diagrams. Parametric conditions for this new oscillatory regime are identified by extending the criticality condition developed by Frank-Kamenetskii for the effect of reactant consumption in diffusive systems to include the effects of both natural and forced convection.

1 Introduction

Thermal combustion occurs when a chemical reaction takes place under conditions of progressive self-acceleration due to heat accumulation. When the rate of heat generation in such a system overcomes the rate of heat loss, it becomes unstable and an explosion (or ignition) occurs. Explosive chemical reactions have been widely studied for approximately 80 years. The original works of Semenov [1] and Frank-Kamenetskii [2] considered solely thermal effects in a well-mixed fluid and in a purely conductive system, respectively. On the one hand, Semenov found that a system explodes when the Semenov number, $\psi = k_0 a_0^n qE/(\chi S_v RT_0^2)$, exceeds the critical value of e^{-1} [1]. On the other hand, for cases where thermal conduction prevails, Frank-Kamenetskii [2] determined critical values of a dimensionless parameter, $\delta = L^2 k_0 a_0^n qE/(\kappa\rho_0 C_p RT_0^2)$, often called the Frank-Kamenetskii number, above which a system explodes. This critical value depends on the geometry of the system, being $\delta_{cr} = 3.32$ for a sphere, 2.00 for a cylinder and 0.88 for parallel plates [2].

When an exothermic chemical reaction occurs in a sufficiently large vessel, in a fluid under normal gravity, the heat release induces temperature gradients in the fluid which in turn can lead to motion, i.e., natural convection. The interaction between exothermic chemical reaction and natural convection has been studied by a number of authors for a simple one-step reaction model occurring in different reactor geometries, including parallel plates [3], horizontal cylinder [3,4], horizontal square prism [5] and sphere [6,7].

While natural convection is a relevant phenomenon to consider in industry as it can develop in any static vessel containing fluids, most industries require further motion (forced convection) in order to achieve good mixing or to move fluids within the industrial process. Mixing often accomplished by the use of jet-stirred reactors (JSRs), particularly for highly exothermic reactions such as chlorination, hydrodealkylation, nitration, and combustion [8]. Wasewar [9] presented a comprehensive review on the numerical and experimental work made on jet-stirred reactors (JSRs). Very few studies have been carried out for laminar flows (e.g., the studies of Fox and Gex [10], Lane and Rice [11]) and other studies are restricted to inert systems or to combustion processes with very good mixing [12–16].

Realistically, the effects of both natural and forced convection, often denominated "mixed convection", are almost always simultaneously present in systems. Thus, it is essential to understand how these phenomena interact with each other and the other thermokinetic mechanisms taking place. Although studies in vertical tubes were abundant [17,18], the three-dimensional numerical investigation of mixed convection in open reactors was only first presented by Arquis *et al.* [19], who simulated a spherical vessel with an inlet and outlet placed on directly opposite sides along the equator. In this work, the pa-

[a] *Department of Chemical Engineering and Biotechnology, University of Cambridge, Pembroke St., Cambridge, CB2 3RA, UK. E-mail: sssc1@cam.ac.uk*
[b] *School of Chemistry, University of Leeds, Leeds, LS2 9JT, UK.*
‡ Present address: Genesis Oil and Gas Consultants Ltd., 1 St. Paul's Churchyard, London, EC4M 8SH, UK.

Table 1 Nomenclature

a	concentration of chemical species A
a'	dimensionless concentration of A, $a' = a/a_s$
a_0	initial concentration of species A
a_s	concentration scale, $a_s = a_0$
C_p	specific heat at constant pressure
C_v	specific heat at constant volume
D_A	diffusion coefficient of species A
E	activation energy
g	acceleration due to gravity
$\underline{g}$	acceleration vector due to gravity
k	kinetic constant for first-order reaction $A \rightarrow B$
L	reactor radius
Le	Lewis number, $Le = \kappa/D_A$
n	reaction order
p	pressure
p'	dimensionless pressure, $p' = (p - p_0)/(\rho_0 U^2)$
Pr	Prandtl number, $Pr = \nu/\kappa$
q	exothermicity of reaction
r	radial position
r'	dimensionless radial position, $r' = r/L$
R	universal gas constant
Ra	Rayleigh number, $Ra = \beta g L^3 \Delta T/(\kappa\nu)$
S_v	surface area per unit volume
t	time
t'	dimensionless time, $t' = tU/L$
T	temperature
T_0	constant wall temperature
T'	dimensionless rise in temperature, $T' = (T - T_0)/\Delta T_s$
$\underline{u}$	velocity vector
$\underline{u}'$	dimensionless velocity vector, $\mathbf{u}' = \mathbf{u}/U$
U	velocity scale, $U = (\beta g \Delta T_s L)^{1/2}$
Z	pre-exponential factor in Arrhenius expression for k
β	thermal expansion coefficient, $\beta = 1/T$
δ	Frank-Kamenetskii's parameter, $\delta = L^2 k_0 c_0^n qE/(\kappa\rho_0 C_p R T_0^2)$
Δt	timestep
ΔT_s	temperature increase scale, $\Delta T_s = RT_0^2/E$
η	$\eta = \Delta T_s/T_0 = RT_0/E$
κ	thermal diffusivity
ν	kinematic viscosity
ρ	density
τ_D	timescale for diffusion
τ_{FC}	timescale for forced convection
τ_{NC}	timescale for natural convection
τ_H	timescale for the exothermic reaction to heat the fluid by ΔT_s
τ_R	timescale for consumption of reactant
χ	heat transfer coefficient
ψ	Semenov number, $\psi = k_0 a_0^n qE/(\chi S_v R T_0^2)$
ω	dimensionless parameter for the effect of reactant consumption
List of subscripts	
0	properties at initial conditions
cr	properties at critical conditions
s	scaling properties
z	conditions related to the vertical direction

rameter $Ra/(Re_i^2 Pr)$ was used to measure the relative intensity of natural and forced convection and to estimate the temperature distribution of the bulk fluid. Here Ra is the Rayleigh number, Re_i is the Reynolds number, measured at the inlet, and Pr is the Prandtl number.

More recently, Liu and Cardoso [20] studied the effects of combined natural and forced convection on a spherical vessel with constant wall temperature and with a simple one-step, n-th order, exothermic reaction taking place without reactant consumption. They considered, as in the work of Arquis *et al.* [19], an input and output at the top and bottom of the vessel, respectively, with a ratio of the inlet and outlet diameter to that of the reactor of 0.05. For the first time, the behaviour of thermal ignition in such systems was addressed and, by the use of timescales to quantify all the transport mechanisms occurring, a new three-dimensional regime diagram was presented, in which the axes represented the relative magnitudes of diffusion of heat, buoyancy and forced convection. Interestingly, Liu and Cardoso [20] found that stronger heat transport mechanisms did not necessarily lead to more stable systems. Instead, they observed a region where a balance between natural and forced convection unexpectedly promoted explosion for systems that would otherwise be stable in the presence of natural or forced convection alone. Liu and Cardoso [20] also reported the appearance of oscillatory behaviour under certain conditions of moderate natural and forced convection and described it briefly, neglecting reactant consumption effects.

The present work is concerned with a simple, one-step, exothermic reaction with reactant consumption in the presence of both natural and forced convection. Using non-dimensionalised conservation equations with timescales for each kinetic and transport phenomena, the behaviour of the system is described using regime diagrams. The oscillatory behaviour is further investigated and the effects of reactant consumption are considered. A new prediction of the parametric conditions for oscillatory behaviour is sought, taking the reactant consumption effects into account.

2 Theoretical analysis

A simple, one-step kinetic model ($A \xrightarrow{k} B$) is considered for a gas in a spherical vessel with radius L. The reaction is assumed to be first-order ($n = 1$) and exothermic ($q > 0$), with activation energy greater than zero ($E > 0$). A stream of pure reactant A is injected at the top of the reactor at a constant flow rate, inducing forced convection in the system. In order to maintain the vessel's pressure, there is an outflow with the same constant flow rate at the bottom of the vessel. The two-dimensional geometry can be seen in fig. 1.

2.1 Governing equations

It is possible to describe this system by a set of governing equations, particularly by the equations of conservation of species A, energy, momentum and continuity:

$$\frac{\partial a}{\partial t} + \underline{u} \cdot \nabla a = D_A \nabla^2 a - ka, \qquad (1)$$

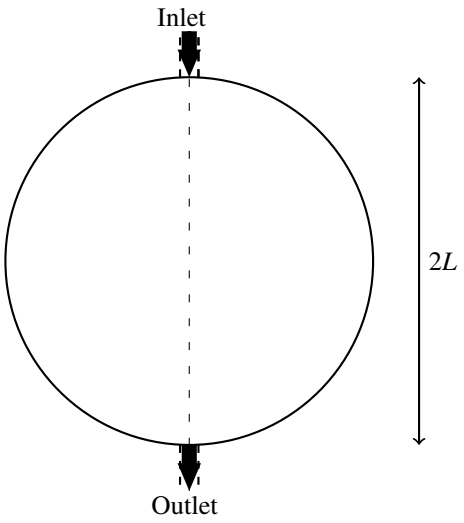

Fig. 1 Axi-symmetric reactor geometry.

$$\frac{C_v}{C_p}\frac{\partial T}{\partial t}+\underline{u}\cdot\nabla T=\kappa\nabla^2 T+\frac{qk}{\rho_0 C_p}a, \tag{2}$$

$$\frac{\partial \underline{u}}{\partial t}+\underline{u}\cdot\nabla\underline{u}=-\frac{1}{\rho_0}\nabla(p-p_0)+\nu\nabla^2\underline{u}+\frac{\rho-\rho_0}{\rho_0}\underline{g}, \tag{3}$$

$$\nabla\cdot\underline{u}=0. \tag{4}$$

The notation is defined in table 1. The fluid is assumed to be incompressible and its density is taken to be that of the reference state, ρ_0, in all terms except in the buoyancy term in the momentum equation (Boussinesq approximation)[21]. The density of the fluid in this term is assumed to vary linearly with temperature as

$$\rho=\rho_0[1-\beta(T-T_0)]. \tag{5}$$

These approximations are valid whenever the increase in temperature in the system is small compared to the system's initial temperature, T_0[22].

The temperature of the vessel is held constant at T_0 and the species flux and fluid velocity are both null at the wall, so that

$$T=T_0;\ \nabla a=0;\ \underline{u}=0\ \text{ at }\ r=L,\ \forall\, t. \tag{6}$$

At the inlet, a stream of pure reactant A is injected downwards at a constant temperature and a parabolic velocity profile is assumed. Thus, the inlet conditions can be described by

$$T=T_0;\ a=a_0;\ u_z=2u_{ave,i}\left[1-\left(\frac{r_{i/o}}{L_{i/o}}\right)^2\right]\ \text{at the inlet, }\forall\, t, \tag{7}$$

where subscript 'z' is associated with the vertical direction of the vessel, $u_{ave,i}$ is the average velocity at the inlet, $r_{i/o}$ is the radial coordinate in the inlet tube and $L_{i/o}$ is the radius of the inlet tube, which is the same for the outlet. The outlet tube is considered to be long enough so that the temperature, concentration and velocity profiles develop fully and the laminar conditions prevail. Hence, if x_z is considered to be the spatial coordinate in the vertical direction, the outlet boundary conditions are:

$$\frac{\partial T}{\partial x_z}=0;\ \frac{\partial a}{\partial x_z}=0;\ \frac{\partial u_z}{\partial x_z}=0\ \text{at the outlet, }\forall\, t. \tag{8}$$

At $t=0$, the temperature is considered to be spatially uniform and the fluid is taken to be stationary and the concentration of A in the reactor is set as a_0, so that

$$T=T_0;\ a=a_0;\ \underline{u}=0\ \text{ at }\ t=0,\ 0<r<L. \tag{9}$$

2.2 Scaling analysis

The concentration of species A, a, temperature, T, velocity, $\underline{u}$, radial position, r, time, t, and pressure, p, can be non-dimensionalised as

$$a'=\frac{a}{a_s},\ T'=\frac{T-T_0}{\Delta T_s},\ \underline{u}'=\frac{\underline{u}}{U},\ r'=\frac{r}{L},\ t'=\frac{U}{L}t,\ p'=\frac{p-p_0}{\rho_0 U^2}, \tag{10 a–f}$$

with

$$a_s=a_0,\Delta T_s=\frac{RT_0{}^2}{E}\ \text{and}\ U=(\beta g\Delta T_s L)^{1/2}. \tag{11 a–c}$$

Timescales for heat transfer by conduction, τ_D, by natural convection, τ_{NC}, and exothermicity, τ_H, can be defined as

$$\tau_D=\frac{L^2}{\kappa},\ \tau_{NC}=\frac{L}{U}\ \text{and}\ \tau_H=\frac{\rho_0 C_p\Delta T_s}{a_s q k_0}. \tag{12 a–c}$$

Moreover, the timescale for consumption of reactant of the first-order reaction, τ_R, and the timescale for forced convection, τ_{FC}, can by described by

$$\tau_R=\frac{1}{k_0}\ \text{and}\ \tau_{FC}=\frac{L^3}{L_{i/o}^2 u_{ave,i}}. \tag{13 a,b}$$

Substituting these timescales and variables in the governing equations, the dimensionless equations become:

$$\frac{\partial a'}{\partial t'}+\underline{u}'\cdot\nabla' a'=\frac{1}{Le}\frac{\tau_{NC}}{\tau_D}\nabla'^2 a'-\frac{\tau_{NC}}{\tau_R}e^{\frac{\phi T'}{1+\eta T'}}a', \tag{14}$$

$$\frac{1}{\gamma}\frac{\partial T'}{\partial t'}+\underline{u}'\cdot\nabla' T'=\frac{\tau_{NC}}{\tau_D}\nabla'^2 T'+\frac{\tau_{NC}}{\tau_H}e^{\frac{\phi T'}{1+\eta T'}}a', \tag{15}$$

$$\frac{\partial \underline{u}'}{\partial t'}+\underline{u}'\cdot\nabla'\underline{u}'=-\nabla' p'+\frac{\tau_{NC}}{\tau_D}Pr\nabla'^2\underline{u}'-\left(\frac{\tau_{NC}}{\tau_D}\right)^2 RaPrT'\frac{\underline{g}}{g}, \tag{16}$$

$$\nabla' \cdot \underline{u}' = 0, \tag{17}$$

where γ, Le, Pr and Ra are, respectively, the heat capacity ratio, Lewis, Prandtl and Rayleigh numbers.

The initial and boundary conditions can then also be made dimensionless:

$$T' = 0;\ \nabla' a' = 0;\ \underline{u}' = 0 \ \text{ at } \ r' = 1,\ \forall\, t', \tag{18}$$

$$T' = 0;\ a' = 1;\ u'_z = 2\frac{\tau_D}{\tau_{FC}}\left(\frac{L}{L_{i/o}}\right)^2\left(1 - {r'_{i/o}}^2\right) \text{ at the inlet, } \forall\, t', \tag{19}$$

$$\frac{\partial T'}{\partial x'_z} = 0;\ \frac{\partial a'}{\partial x'_z} = 0;\ \frac{\partial u'_z}{\partial x'_z} = 0 \text{ at the outlet, } \forall\, t', \tag{20}$$

$$T' = 0;\ a' = 1;\ \underline{u}' = 0 \ \text{ at } \ t' = 0,\ 0 < r' < 1. \tag{21}$$

This system is therefore characterised by the following nine dimensionless groups:

$$Le,\ \eta,\ \gamma,\ Pr,\ \frac{L}{L_{i/o}},\ \frac{\tau_D}{\tau_{FC}},\ \frac{\tau_H}{\tau_D},\ \frac{\tau_H}{\tau_{NC}} \text{ and } \frac{\tau_H}{\tau_R}. \tag{22 a–i}$$

The first five groups are defined once the chemical system, geometry of the vessel and initial temperature are fixed and the system can then be described by the four ratios of timescales for the different transport phenomena.

3 Numerical method

The four governing equations (1)-(4) were solved numerically for a spherical reactor with an inlet at the top and outlet at the bottom with equal radius of 0.0032 m, 20 times smaller than the radius of the reactor, $L = 0.064$m. The outlet tube was 0.2 m long, so that the fluid at the exit exhibited a laminar behaviour, with a parabolic velocity profile and a uniform temperature and concentration distribution in the vertical direction. The finite-element solver Fastflo[23] was used with an algorithm as described previously[7,20,24–26]. The method of Picard of successive approximations was employed for linearisation, combined with a backward Euler time-stepping scheme, and the momentum and continuity equations were coupled using the Augmented-Lagrangian method[23]. Owing to the axisymmetric geometry, a semi-circular mesh of about 7500 elements was applied and a timestep of 0.01 s was used. The reaction analysed was the thermal decomposition of pure azomethane $\left(CH_3N_2CH_3\right)$ and the physico-chemical parameters were chosen in agreement with previous experimental[27] and numerical[20] work, as follows. The temperatures of the inflow and the vessel wall were maintained at the initial temperature $T_0 = 636.2$ K. The initial concentration of reactant was $a_0 = 0.37$ mol m^{-3} (corresponding to $p \approx 0.02$ bar). The order of reaction, n, was assumed to be 1. The physico-chemical properties were: $C_p = 2250$ J kg^{-1} K^{-1}, $k_0 = 0.0159$ s^{-1}, $E/R = 23280$ K, $Pr = Le = 1$ and $\gamma = 1.018$[20,27]. At the wall, both fluid velocity and flux of chemical species were set as zero. For convergence purposes, the relative velocity change between consecutive iterations, summed over all mesh nodes, was kept under 0.01 and continuity, equation (4), was satisfied within 1×10^{-5} s^{-1}. For each simulation, the values of τ_D/τ_{FC}, τ_H/τ_R, τ_H/τ_D and τ_H/τ_{NC} were varied by changing the average velocity at the inlet ($u_{ave,i}$), the acceleration of gravity (g), the diffusivity of the fluid (κ) and the exothermicity of reaction (q). The values of Ra, which vary with τ_D/τ_{FC}, τ_H/τ_D and τ_H/τ_{NC}, were kept under 10^6 to maintain the laminar regime of the flow.

4 Results and discussion

4.1 Regime Diagram

Simulations were performed for several reactant consumption rates and forced convection intensities; results will be shown for systems with $\tau_H/\tau_R = 0$, 0.02, 0.05, 0.10 and 0.15, and $\tau_D/\tau_{FC} = 0$, 1.25, 2.5, 5.0, 10.0 and 20.0. The same physico-chemical parameter values were used for cases with $\tau_H/\tau_R = 0$ (without solving the mass balance equation) and for $\tau_H/\tau_R = 0.02$, so the difference between these results is due to neglecting reactant consumption in this system. For consistency with results of Liu and Cardoso[20], two-dimensional diagrams of τ_H/τ_D-τ_H/τ_{NC} are presented for each value of τ_D/τ_{FC} and several τ_H/τ_R magnitudes. To represent each explosion boundary, the results of 50 to 80 simulations were used. Ignition was considered to take place when the dimensionless temperature attained a value of 5, since this was shown to be an appropriate explosion criterion for closed systems with a first-order reaction and reactant consumption[7].

Figure 2a shows the two-dimensional regime diagram for a system without forced convection, with the explosion boundaries for several reactant consumption rates. Since there is no forced convection, this case is equivalent to a closed system. Therefore, when reactant consumption is absent, the results are equivalent to those of Liu *et al.*[7], where the Frank-Kamenetskii limit for a simple $A \rightarrow B$ reaction coincides with the τ_H/τ_D axis. In fact, $\tau_H/\tau_D = 0.30$ is equivalent to the inverse of Frank-Kamenetskii's critical parameter for a sphere ($\delta_{cr} = 3.32$), and the remaining results in fig. 2a also match those of Liu *et al.*[7]. It is observed that when the rate of fuel consumption increases (higher τ_H/τ_R), the system becomes more stable, regardless of the intensity of the exothermicity of reaction and the natural convection present in the vessel. The reduction of the explosive region due to reactant consumption is slightly more pronounced for negligible natural convection than for higher τ_H/τ_{NC}. With weak natural and forced convection, the fluid is almost stagnant and the temperature rise occurs in the centre of the vessel, with less heat removal through

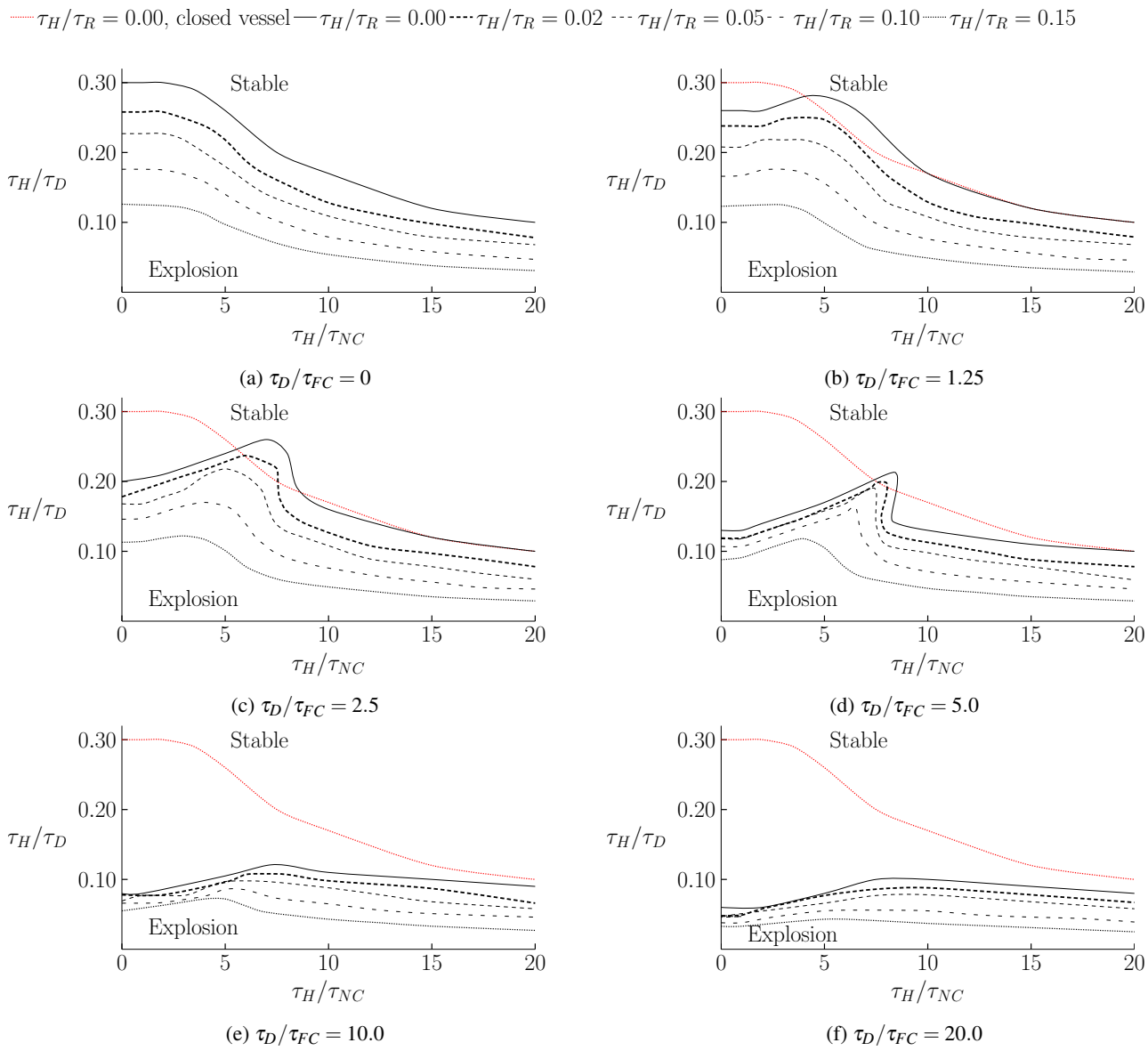

Fig. 2 Two-dimensional regime diagram for different forced convection intensities. The results of Liu and Cardoso [20] have been corrected for a perfect spherical geometry.

the walls than in cases with stronger natural convection, where the hot region travels towards the walls of the vessel. Hence, a lower exothermicity (higher τ_H/τ_D) is sufficient to lead systems without natural convection to explosion, but the time to explosion is longer than that of explosive cases with strong natural convection. With the increase of the global temperature and the time for reaction, which allows more fuel consumption, the stabilising effect of reactant consumption becomes more pronounced on the left-hand side of the regime diagram than for systems with higher buoyant effects.

By inducing motion in the vessel, a balance between natural and forced convection can cause the fluid to develop a stagnant region near the centre of the vessel which quickly heats up and favours explosion for conditions that would otherwise lead to a stable reaction [20]. This is shown in fig. 2b by the difference between the red dotted explosion boundary of the closed vessel without reactant consumption and the explosion boundary for systems with weak forced convection ($\tau_D/\tau_{FC} = 1.25$), also without reactant consumption. The depletion of reactant acts as a stabiliser to the system, similarly to the closed system. One difference between a closed system and an open system with weak or moderate forced convection lies in the balance

between natural and forced convection that favours explosive behaviour, as Liu and Cardoso [20] observed. This balance is perturbed by reactant consumption since the stagnant region does not heat up as much nor as quickly as in cases without reactant depletion. This results in a reduction of the peak of the explosive boundary for which natural and forced convection are counterbalanced. For stronger reaction consumption rates, the protuberance of the boundary eventually disappears, as can be seen by observing the explosion limit of cases with $\tau_H/\tau_R = 0.15$ in fig. 2b. In other words, sufficient reactant consumption hinders the equilibrium between buoyant and induced motion of the fluid.

Figures 2c to 2f show the effect of reactant consumption on the explosion boundaries of systems with increasing strengths of forced convection. Even though the behaviour of the fluid motion can differ significantly for different forced convection intensities, as minutely described by Liu and Cardoso [20], the generic effect of depletion of fuel remains unchanged, hampering explosion. The reduction of the region where natural and forced convection are balanced is always greater for higher consumption rates. However, for cases where this equilibrium is stronger (i.e. $\tau_D/\tau_{FC} = 2.5$ and 5.0), higher rates of consumption of A are needed to fully suppress the protrusion of the explosion boundary.

For cases with strong forced convection ($\tau_D/\tau_{FC} = 10.0$ and 20.0) the reduction of the explosive region due to fuel consumption is relatively uniform for all magnitudes of natural convection but less pronounced than that of cases with weaker forced convection. When the inlet stream is sufficiently fast, a channel of cold fluid develops in the centre of the reactor, with a lower residence time than the bulk fluid in the reactor [20]. As the cold injected stream is entirely species A, there is a bypass of fuel through the vertical axis of the reactor, without sufficient time for significant reaction to take place and, consequently, with a negligible temperature increase. As a consequence, the effects of reactant consumption are not as pronounced as in cases with lower forced convection (lower τ_D/τ_{FC}). Figures 2b to 2f show this tendency. The cases for which thermal and convective effects are very strong approach the limit of the laminar regime and the transition to turbulent flow. Hence, special care is needed to interpret results near the bottom right region of the regime diagram, for very strong forced convection effects, as accuracy might be compromised.

4.2 Oscillatory Behaviour for Moderate Forced Convection

Liu and Cardoso [20] reported the existence of cyclic behaviour of the temperature and flow fields under a limited range of conditions for open systems with moderate forced convection and without reactant consumption. In systems where forced convection plays an important role, the position of the hottest region can vary significantly. Therefore, if one wants to identify oscillations due to thermokinetic effects, it is not appropriate to evaluate the oscillatory behaviour of a variable, e.g. temperature or concentration, at a specific point in the vessel. These values can in fact display oscillatory behaviour but this is indiscernible from the oscillations of the location of the maximum temperature or minimum concentration of reactant, i.e. flow oscillations. By observing the maximum temperature and minimum concentration of A, it is often possible to detect the oscillatory behaviour of these parameters, regardless of their spatial location. However, it was observed that in some cases the extreme values of these variables do not encompass the oscillatory behaviour but that oscillations occur at intermediate values of both temperature and concentration of A. Furthermore, these physical behaviours are difficult to measure practically in vessels. Following the evolution of the velocity in the centre of the reactor can help to identify the oscillatory behaviour of the fluid flow but it does not give immediate feedback about the temperature or fuel concentration evolution.

Thus, monitoring the heat flux through the reactor walls becomes a more attractive and appropriate alternative to evaluate if the system exhibits oscillatory behaviour in temperature, concentration and/or flow fields since the flux depends on the system's temperature and on the position and size of the hot region relative to the wall. In non-explosive cases in closed systems, the heat flux through the wall is expected to have one of two behaviours: either it rises monotonically to a steady state for cases with weak exothermicity and reactant consumption, or it rises to a maximum while heat is released by reaction, and subsequently falls to a steady-state value, due to reactant consumption and heat removal taking place. Since there is no thermal feedback under these conditions, oscillations in temperature and concentration are not observed even though a single peak in the heat flux can be detected. In order to distinguish this behaviour from the damped and sustained oscillatory behaviour induced by the presence of forced convection, oscillatory cases will from now on be defined as the ones where heat fluxes exhibit at least two relative maxima during reaction time. Since Liu and Cardoso [20] reported the existence of more oscillatory cases for systems with $\tau_D/\tau_{FC} = 5.0$ than for any other forced convection intensity analysed in their work, the following sections will focus on these conditions.

To study the effects of the different thermokinetic phenomena on the oscillatory behaviour, several cases will be examined in detail through the following sections. The effects of fuel consumption will be examined through cases I to III, the natural convection effects will be discussed for cases IV to VI and the impact of the thermal effect will be analysed for cases VII to IX. Table 2 summarises the parametric conditions for all these cases.

Table 2 Governing parameters for cases I to IX.

	$\frac{\tau_D}{\tau_{FC}}$	$\frac{\tau_H}{\tau_R}$	$\frac{\tau_H}{\tau_{NC}}$	$\frac{\tau_H}{\tau_D}$	κ ($m^2\ s^{-1}$)	q ($kJ\ mol^{-1}$)	$u_{ave,i}$ ($m\ s^{-1}$)	g ($m\ s^{-2}$)
Case I	5.0	0	9.0	0.16	5.70×10^{-4}	124.28	17.81	143.49
Case II	5.0	0.05	9.0	0.16	2.09×10^{-4}	45.46	6.52	19.20
Case III	5.0	0.10	9.0	0.16	1.04×10^{-4}	22.73	3.26	4.80
Case IV	5.0	0.05	7.0	0.16	2.09×10^{-4}	45.46	6.52	11.62
Case V	5.0	0.05	11.0	0.16	2.09×10^{-4}	45.46	6.52	28.68
Case VI	5.0	0.05	13.0	0.16	2.09×10^{-4}	45.46	6.52	40.06
Case VII	5.0	0.05	9.0	0.12	1.56×10^{-4}	45.46	4.89	19.20
Case VIII	5.0	0.05	9.0	0.14	1.82×10^{-4}	45.46	5.70	19.20
Case IX	5.0	0.05	9.0	0.18	2.35×10^{-4}	45.46	7.33	19.20

4.2.1 Reactant Consumption Effects Figure 3 shows the evolution of the temperature fields for case I, without reactant consumption. At $t = 0.5$ s the heating up by reaction is already evident, favouring buoyancy. The vertical velocity at the centre of the reactor at this moment is negative, which indicates that the fluid is moving downwards owing to the inlet stream forces. However, natural convection counteracts the forced convection motion, as can be seen by the increasingly negative streamlines coming gradually closer to the centre ($t = 1.0$ s), decelerating the downflow, until it eventually reaches a nearly stagnant state, at $t = 1.17$ s, when the vertical velocity is zero at the centre of the vessel. This favours the heating of the fluid and enhances natural convection even further, as shown at $t = 1.5$ s, where the hot region is higher in the vessel and the negative toroidal streamlines are denser than in the preceding moments. Nonetheless, the effects of the cold inlet stream flatten the hot region and so the temperature rise is greater towards the side of the reactor, slowing down the upward flow at the vertical axis and gradually dividing the hot region. The streamlines at $t = 2.5$ s show this deceleration of the fluid at the centre, while the hot region on the sides continues to moves up. The flow at the centre is reversed again at $t = 2.66$ s. In fact, at $t = 3.0$ s, the streamlines show a different behaviour: the fluid at the centre moves downwards with increasing speed, shifting the hot region away from the centre, to the bottom of the vessel.

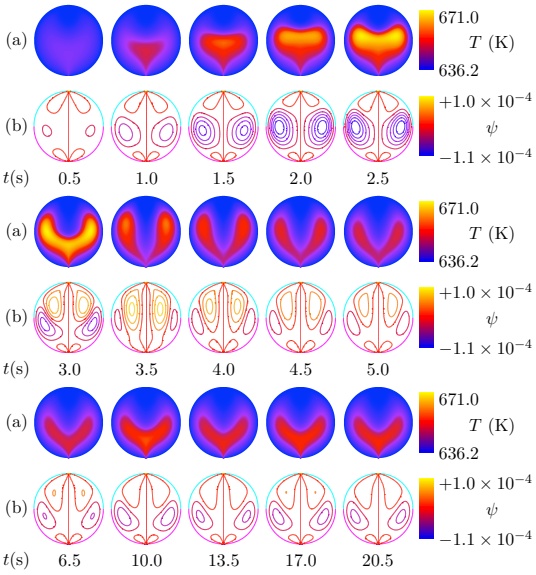

Fig. 3 Evolution of the fields of (a) temperature and (b) streamlines for case I, with $\tau_D/\tau_{FC} = 5.0$, $\tau_H/\tau_R = 0$, $\tau_H/\tau_D = 0.16$ and $\tau_H/\tau_{NC} = 9.0$.

The blue toroidal vortices at the bottom indicate that buoyancy shifts the hot fluid up and towards the wall where it cools and proceeds to move downwards close to the wall. Near the top, two vortices develop on each side of the reactor, pushing the fluid down at the vertical axis. During this descent, the fluid heats up slightly by reaction and, consequently, moves diagonally up towards the wall and shifts to the centre again due to the spherical geometry of the vessel. While this motion occurs, the removal of heat through the walls is dominant and the temperature decreases sharply along the vertical axis, allowing the fluid to speed up further at the centre, towards the bottom of the vessel. At $t = 3.5$ s, the vertical velocity at the centre reaches its maximum negative value, and the bottom vortices nearly disappear, overcome by the motion of the top vortices. Meanwhile, as can be seen from $t = 4.0$ to 6.5 s, the heat generation is favoured once again at the bottom of the reactor, which in turn triggers natural convection, slows the downflow at the centre and enhances heat removal through the wall. After 10 seconds of reaction, heat removal overcomes its generation and temperature at the bottom of the vessel starts decreasing gently until the exothermicity is sufficient to increase the temperature once more. The spatiotemporal change in temperature after 17 seconds is so subtle that it is barely

observable in fig. 3. These phenomena occur repeatedly until a steady state is achieved, at $t \approx 45.0$ s.

Figure 4 shows the evolution of temperature, concentration and streamlines fields for case II, with weak reactant depletion ($\tau_H/\tau_R = 0.05$), analogous to the case without reactant consumption. Similar to case I, the fluid starts heating up shortly after reaction begins, initiating the movement due to natural convection and counterbalancing the forced convection motion at the centre at $t = 3.18$ s. At $t = 5.0$ s the upflow can be detected by the very dense, negative streamlines forming vortices approximately at the equator and very near the centre of the reactor. The consumption of fuel is also visible at this moment, forming a darker region (lower concentration) at the centre. After 7.5 seconds of reaction, the upward flow slows down as the hot region spreads sideways and the depletion of fuel progresses, still at a higher rate at the centre of the reactor than in the bulk of the vessel. At $t = 8.66$ s the flow reverses at the centre and it can be seen at $t = 10.0$ s that the top vortices with positive streamlines stretch down to the centre of the vessel, indicating a downwards flow at this point. The

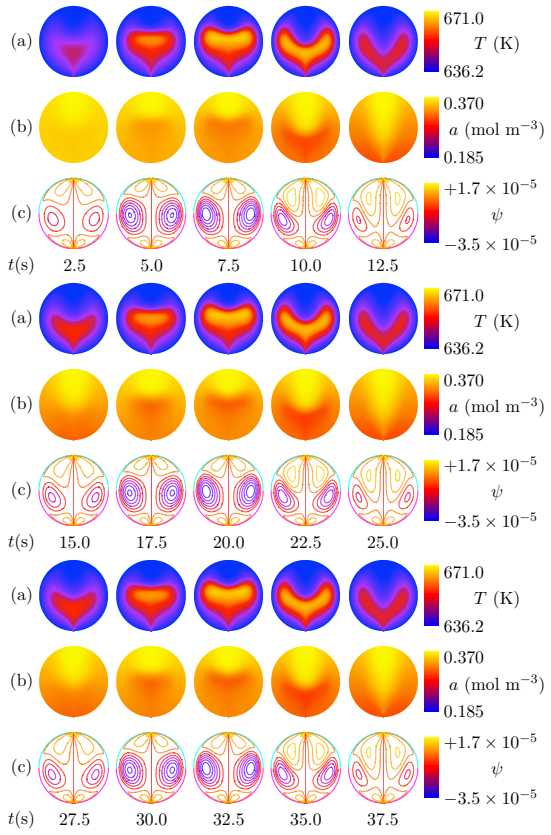

Fig. 4 Evolution of the fields of (a) temperature, (b) reactant concentration and (c) streamlines for case II, with $\tau_D/\tau_{FC} = 5.0$, $\tau_H/\tau_R = 0.05$, $\tau_H/\tau_D = 0.16$ and $\tau_H/\tau_{NC} = 9.0$.

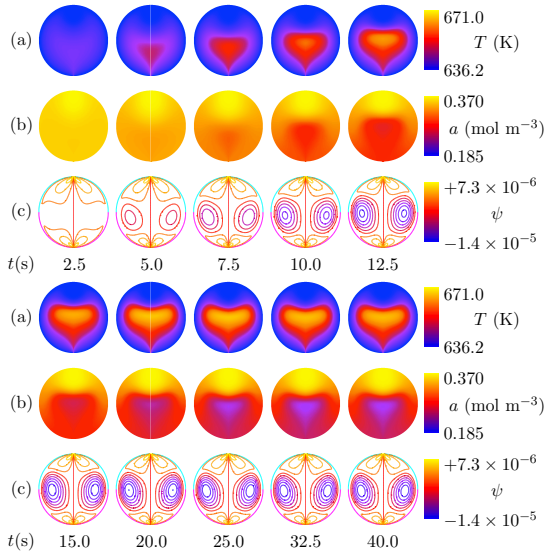

Fig. 5 Evolution of the fields of (a) temperature, (b) reactant concentration and (c) streamlines for case III, with $\tau_D/\tau_{FC} = 5.0$, $\tau_H/\tau_R = 0.10$, $\tau_H/\tau_D = 0.16$ and $\tau_H/\tau_{NC} = 9.0$.

hot region is deformed into a v-shape as the cold inlet stream shifts the hot region to the bottom and sides of the reactor, enhancing the heat loss through the walls, which consequently decreases the bulk temperature of the reactant. As the inlet stream contains only species A, the lower concentration region also moves down in the vessel and has a similar shape to that of the hot region, as it would be expected. The downward flow reaches its maximum velocity about 12.5 seconds after the start of the reaction, with the cold stream of pure fuel nearly bypassing the reactor and favouring the heating by reaction at the bottom of the reactor, visible at $t = 15.0$ s. Once again, natural convection gains strength and the whole chain of events repeats. As the natural and forced convection motions are of the same order of magnitude and balanced by the heat removal of the system, the temperature, concentration of A and fluid flow oscillate indefinitely with constant amplitudes and frequency, as shown by the similarity of fields at moments $t = 12.5$ to 25.0 s and $t = 25.0$ to 37.5 s. Comparing this case to case I, in fig. 3, it is evident that the reactant depletion delays the temperature rise and promotes further the oscillatory behaviour, under these specific conditions of convection and exothermicity.

The evolution of temperature, fuel concentration and streamlines for case III, with $\tau_H/\tau_R = 0.10$, is displayed in fig. 5. The initial behaviour of this system is analogous to the corresponding cases I and II (with $\tau_H/\tau_R = 0$ and 0.05, respectively), with an even more pronounced delay of the temperature rise and concentration decrease than in case II. As reaction progresses, the high temperature and low concentra-

tion regions develop at the bottom and proceed to move up towards the centre of the vessel, owing to natural convection effects, with a flattened shape at the top due to forced convection. The flow at the centre of the reactor, initially downwards, is reversed at $t = 6.97$ s and the vertical velocity at this point remains positive for all times after this moment, reaching a maximum value at $t = 12.5$ s. Heating by reaction then continues to increase the temperature of the contents of the vessel, subsequently promoting heat removal and, consequently, reducing the velocity of the flow at the centre, as shown between $t = 15$ and 25 s, where the distance between the two toroidal vortices increases. Meanwhile, the concentration of species A continues to gradually decrease at the hot region as demonstrated by the darker region developing in the centre of the reactor. However, the feed of pure reactant through the inlet hinders this drop. After about 32.5 seconds of reaction, all the transport mechanisms attain an equilibrium and both temperature and concentration of A reach a steady state, stabilising the flow as well.

To better understand the difference between cases I to III, the heat fluxes through the wall are plotted against time in fig. 6. The damped oscillatory behaviour of case I and the sustained oscillations of case II are evident in this figure. In all three cases, there is a deceleration of the initial heat flux rise, before it reaches the first peak value. This occurs when buoyancy starts increasing, moving the hot region to the centre, further away from the walls. However, the fluid motion induced by the inlet stream consequently shifts the hot region towards the sides of the reactor, closer to the walls, and this causes a further rise of the heat flux. For cases with increasing reactant consumption rates, the deceleration of the heat flux rise occurs for greater times of reaction since the onset of natural convection is delayed. Table 3 shows the maximum values of the dimensionless temperature for the three cases and the dimensionless time to attain these values for each reaction. The maximum temperature reached in the vessel is reduced and clearly delayed with increasing reactant consumption, as expected. Also, by comparing the stream function scales of figs. 3 to 5, it is observed that the fluid motion is hindered for cases with increasing reactant depletion.

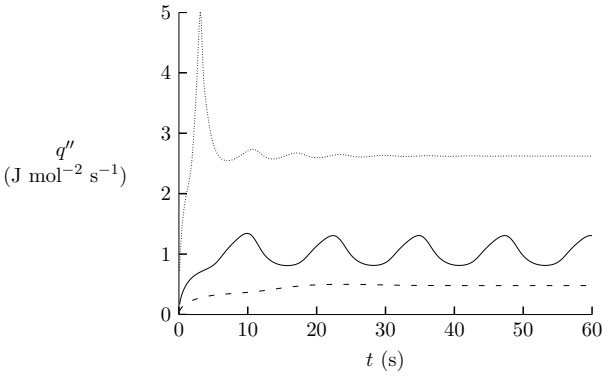

Fig. 6 Evolution of heat fluxes through the wall of the vessel for case I (dotted line), case II (solid line) and case III (dashed line). All cases are for reactions with $\tau_D/\tau_{FC} = 5.0$, $\tau_H/\tau_{NC} = 9.0$ and $\tau_H/\tau_D = 0.16$.

Table 3 Comparison of the maximum dimensionless temperature and dimensionless time to reach the peak temperature for cases I to III.

Case	I	II	III
T'_{max}	2.10	1.88	1.78
$t'_{T_{max}}$	0.39	0.46	0.59

4.2.2 Natural Convection Effects Natural convection plays a significant role on the oscillatory behaviour of the system since it is buoyancy that counterbalances the motion caused by the injection of the cold stream at the top of the vessel. To investigate the effects of natural convection on the oscillatory regime, cases with $\tau_D/\tau_{FC} = 5.0$ and $\tau_H/\tau_R = 0.05$ will be examined for constant values of $\tau_H/\tau_D = 0.16$ and increasing values of τ_H/τ_{NC}. The governing parameters for all cases were previously stated in table 2.

Figure 7 shows the explosive behaviour of case IV. This case is analogous to case II, previously examined in fig. 4, but with weaker natural convection effects ($\tau_H/\tau_{NC} = 7.0$). As in previous cases, the temperature starts rising at the bottom of the vessel, accompanied by reactant depletion, and buoyancy is triggered within the fluid. However, since the natural convection intensity is weaker (lower τ_H/τ_{NC}), it takes longer for the hot region to shift upwards than any of the cases examined so far. The inversion of the flow at the centre occurs only at $t = 4.93$ s, also later than in cases I and II. Owing to the interaction between buoyancy and forced convection the hot region expands further to both sides of the reactor where the cooling by diffusion of colder species from the inlet stream is

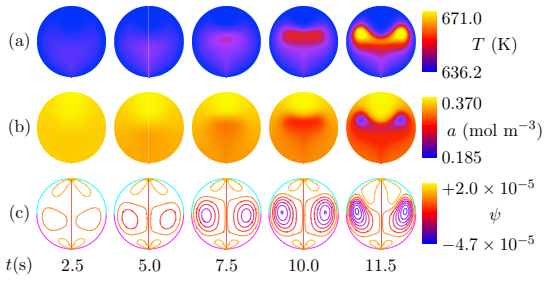

Fig. 7 Evolution of the fields of (a) temperature, (b) reactant concentration and (c) streamlines for case IV, with $\tau_D/\tau_{FC} = 5.0$, $\tau_H/\tau_R = 0.05$, $\tau_H/\tau_D = 0.16$ and $\tau_H/\tau_{NC} = 7.0$.

not so efficient. This allows the fluid to heat up by reaction quite rapidly, leading to explosion at $t = 11.5$ s.

The behaviour of case V is shown in fig. 8. In this case, since convection is stronger than in previous cases, the hot region travels swiftly to the centre of the vessel and starts spreading away from the vertical axis. As heat is readily lost through the walls, the temperature does not rise as high as for cases with weaker natural convection and, for the same reason, the reactant does not deplete as extensively as in cases II or IV. Thus, forced convection counterbalances the upward buoyant flow and reverses the flow at the centre once again, at $t = 5.90$ s. The hot region is pushed downwards and closer to the walls, enhancing heat loss, and the temperature drops to a minimum at $t = 10.0$ s. Heating by reaction continues to occur at the bottom of the vessel, with the feed of pure species A from the injected stream, and reheats the system ($t = 17.5$ s). However, owing to strong buoyancy present in the system, the heat is quickly lost to the surroundings and the fuel is replenished, completing the second oscillation of temperature, concentration and flow at $t = 23.5$ s. The temperature and concentration in the vessel continue to oscillate after this moment, with decreasing amplitude, to become almost unidentifiable (fig. 8). Yet, if one observes time points $t = 23.5$ s and $t = 30.0$ s, the difference in the size of the hot region is indeed recognisable, being slightly larger in the latter.

The evolution of temperature, concentration of A and flow fields for case VI, with $\tau_H/\tau_{NC} = 13.0$, is shown in fig. 9. This case shows an extremely quick development of buoyant flow, deforming the hot region into the v-shape in less than 5 seconds, and promoting immediate heat loss through the walls. In fact, the reaction is so fast that a steady state is attained before $t = 10.0$ s.

Figure 10 compares the temporal evolution of the heat flow through the walls for cases II and IV to VI. This figure clearly shows the transition between the explosive behaviour at $\tau_H/\tau_{NC} = 7.0$ (case IV) to a stable, non-oscillatory behaviour at $\tau_H/\tau_{NC} = 13.0$ (case VI), going through sustained oscillations adjacent to the explosive boundary ($\tau_H/\tau_{NC} = 9.0$, case II) and exhibiting damped oscillations in temperature, concentration and flow for $\tau_H/\tau_{NC} = 11.0$ (case V). The heat fluxes for cases with weaker buoyant effects reach higher values, owing to the higher temperature attained in the vessel. Table 4 shows the maximum values of the dimensionless temperature for cases II and IV to VI and the dimensionless time to attain these values for each reaction. For cases with weaker buoyant effects, the maximum values of temperature and, consequently, the maximum heat flux occur earlier.

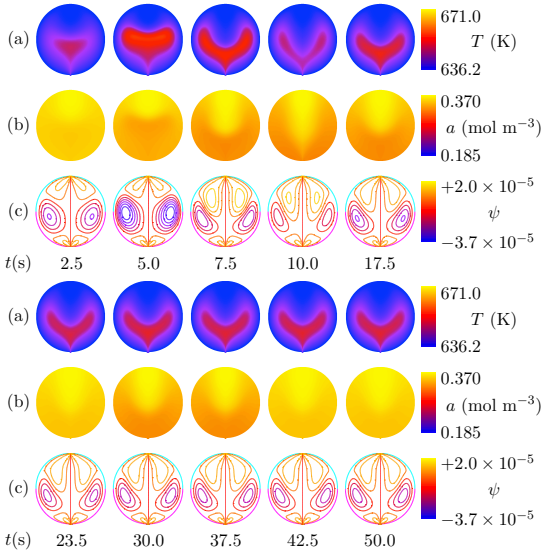

Fig. 8 Evolution of the fields of (a) temperature, (b) reactant concentration and (c) streamlines for case V, with $\tau_D/\tau_{FC} = 5.0$, $\tau_H/\tau_R = 0.05$, $\tau_H/\tau_D = 0.16$ and $\tau_H/\tau_{NC} = 11.0$.

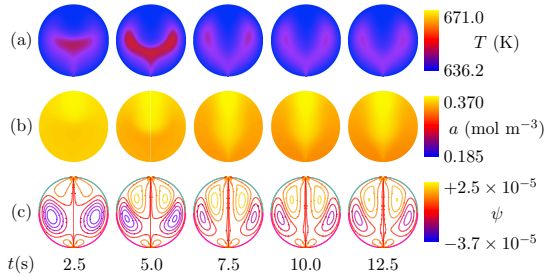

Fig. 9 Evolution of the fields of (a) temperature, (b) reactant concentration and (c) streamlines for case VI, with $\tau_D/\tau_{FC} = 5.0$, $\tau_H/\tau_R = 0.05$, $\tau_H/\tau_D = 0.16$ and $\tau_H/\tau_{NC} = 13.0$.

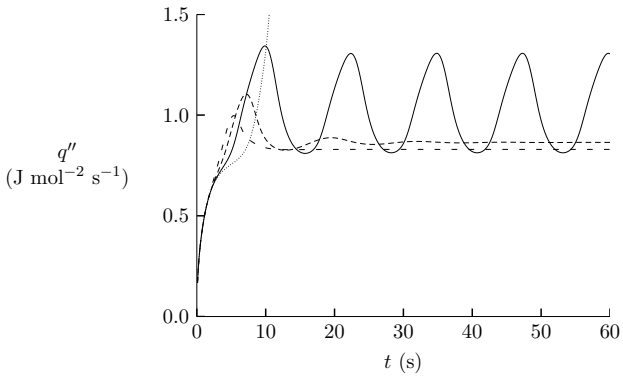

Fig. 10 Evolution of heat fluxes through the wall of the vessel for case IV (dotted line), case II (solid line), case V (densely dashed line) and case VI (loosely dashed line). All cases are for reactions with $\tau_D/\tau_{FC} = 5.0$, $\tau_H/\tau_R = 0.05$ and $\tau_H/\tau_D = 0.16$.

Table 4 Comparison of the maximum dimensionless temperature and dimensionless time to reach the peak temperature for cases II and IV to VI.

Case	IV	II	V	VI
T'_{max}	∞	1.88	1.34	1.05
$t'_{T_{max}}$	-	0.46	0.32	0.21

4.2.3 Thermal Effects Cases located along a vertical line (constant $\tau_H/\tau_{NC} = 9.0$) of the regime diagram for systems with some reactant consumption ($\tau_H/\tau_R = 0.05$), will be compared in this section. The parameters for each case were presented in table 2.

Figure 11 shows the evolution of temperature, fuel concentration and flow motion for case VII, with strong exothermicity. The initial heating of the fluid is clearly seen early on ($t = 1.5$ s), and after 2.5 seconds of reaction the natural convection effects, enhanced by the strong exothermicity, are conspicuous, having reversed the flow at the centre of the vessel. Later, the hot region proceeds to move sideways, allowing the inlet stream to overcome the natural convection motion at the centre, and the reactant is gradually consumed. As the hot fluid approaches the walls, heat removal becomes more effective. Yet, between $t = 5.5$ s and $t = 6.5$ s, there is still a mild increase in temperature owing to the high heat release rate. However, heat flux through the walls compensates heat generation and temperature starts decreasing monotonically throughout the vessel after $t = 6.5$ s, until it reaches a steady-state value, just before $t = 20.0$ s. During this period, the reactant consumption is strongest near the walls, where the temperature remains higher than in the bulk of the fluid. Unexpectedly, the concentration of fuel continues decreasing near the walls, even when the temperature decreases ($t > 6.5$ s). Yet, the concentration field also reaches a steady state at $t \approx 15.0$ s. This reduction in concentration indicates that mass diffusion and temperature effects on the concentration of species are, at this point, negligible when compared to the natural and forced convection motion of the fluid. The stream of species A fed at the top bypasses the vessel without barely reacting and the bulk of the fluid, on the sides, has a larger residence time, reacting more extensively than the axial fluid. Comparing this case to case II, with $\tau_H/\tau_D = 0.16$ (fig. 4), it is visible that, even though the natural convection timescale is the same for both cases, the hot region rises higher in the case with higher exothermicity (case VII). This is due to the fact that the temperature rises more in this case, promoting the buoyant motion within the vessel.

The behaviour of case VIII, with $\tau_H/\tau_D = 0.14$, can be seen in fig. 12. The evolution of temperature, concentration of A and flow is similar to case VII. The striking differences are that the hot region in case VIII does not rise as much and the reactant depletion by the walls is not as extensive as in case VII. These are expected consequences of reducing the thermal effects of the system by increasing the ratio τ_H/τ_D. Another difference in this case is the occurrence of damped oscillations in the three fields shown in fig. 12. Whilst in case VII the

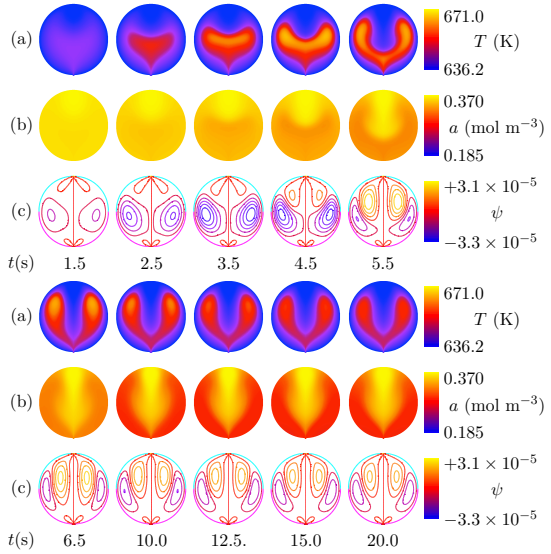

Fig. 11 Evolution of the fields of (a) temperature, (b) reactant concentration and (c) streamlines for case VII, with $\tau_D/\tau_{FC} = 5.0$, $\tau_H/\tau_R = 0.05$, $\tau_H/\tau_D = 0.12$ and $\tau_H/\tau_{NC} = 9.0$.

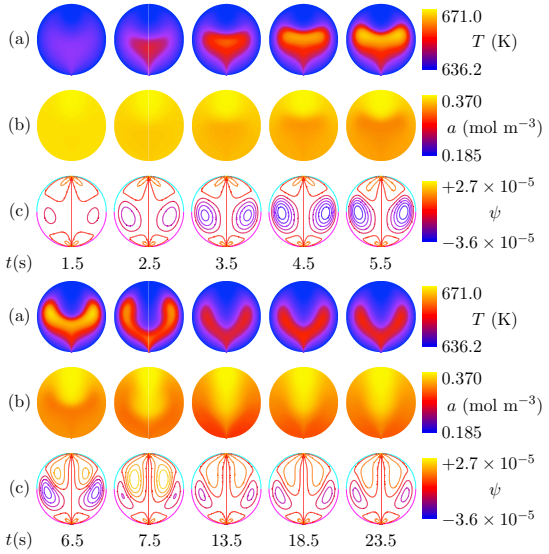

Fig. 12 Evolution of the fields of (a) temperature, (b) reactant concentration and (c) streamlines for case VIII, with $\tau_D/\tau_{FC} = 5.0$, $\tau_H/\tau_R = 0.05$, $\tau_H/\tau_D = 0.14$ and $\tau_H/\tau_{NC} = 9.0$.

temperature decreased monotonically to a steady state after the heat removal through the walls counterbalanced the heat generation of the system, in case VIII the global temperature reduces to a lower value than its steady-state value ($t = 13.5$ s), then rises again to a value slightly above the equilibrium ($t = 18.5$ s) and finally reaches a steady state at $t = 23.5$ s. The oscillations in concentration and flow are less conspicuous but also occur for case VIII.

Increasing the ratio τ_H/τ_D to 0.16 promotes sustained oscillatory behaviour of the temperature, concentration and flow, as previously seen in case II (fig. 4). The behaviour of case IX, with the weakest exothermicity of all cases ($\tau_H/\tau_D = 0.18$), is displayed in fig. 13. The heating of the fluid by reaction starts to take place very slowly, inducing buoyancy within the vessel, so that the hot region rises and spreads sideways. The reactant depletion accompanies the slow evolution of the temperature gradient and the shape of the less concentrated region coincides with that of the hot region for all times. Regarding the flow evolution, as soon as natural convection settles in the vessel, toroidal vortices develop on each side of the reactor that slowly move upwards with the evolution of the hot region. These vortices gain speed and eventually reverse the downflow at the centre of the reactor (at $t = 4.27$ s), allowing the temperature to rise further in this region. Temperature and concentration continue increasing and decreasing monotonically, respectively, and all three fields reach a steady state around $t = 20.0$ s, without any oscillations.

Figure 14 compares the evolution of heat fluxes through the wall for the cases with varying exothermicities. The moment

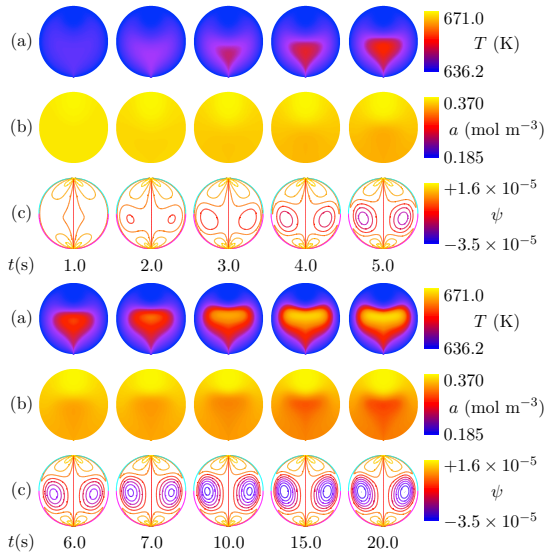

Fig. 13 Evolution of the fields of (a) temperature, (b) reactant concentration and (c) streamlines for case IX, with $\tau_D/\tau_{FC} = 5.0$, $\tau_H/\tau_R = 0.05$, $\tau_H/\tau_D = 0.18$ and $\tau_H/\tau_{NC} = 9.0$.

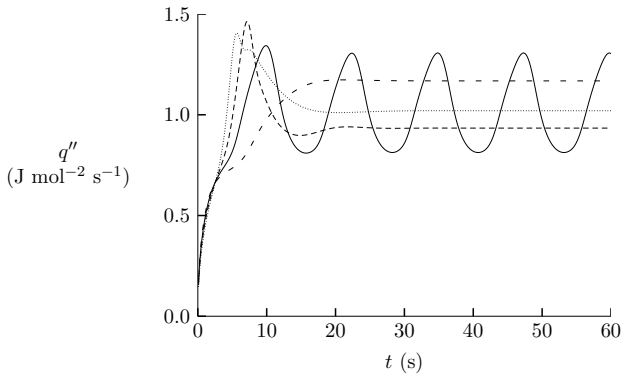

Fig. 14 Evolution of heat fluxes through the wall of the vessel for case VII (dotted line), case VIII (densely dashed line), case II (solid line) and case IX (loosely dashed line). All cases are for reactions with $\tau_D/\tau_{FC} = 5.0$, $\tau_H/\tau_R = 0.05$ and $\tau_H/\tau_{NC} = 9.0$.

when buoyant motion lifts the hot region up towards the centre of the vessel can be seen for all four cases, when the increase of the heat flux is slightly hampered, after only a few seconds of reaction and before the first peak of the heat flux. The heat flux rise accelerates again when the hot region spreads to the sides, closer to the walls. For stronger exothermicity (lower τ_H/τ_D) this acceleration is more pronounced owing to the faster temperature rise to higher values than in the other cases. Observing case VII, with $\tau_H/\tau_D = 0.12$, one can notice a small plateau on the reduction of the heat flux to the steady state. This corresponds to the moment between $t = 5.5$ and 6.5 s, when the temperature in the hot region rises slightly owing to the strong exothermicity of reaction, as noted before.

4.2.4 Oscillatory Regions in the Regime Diagram Liu and Cardoso [20] found cases falling within the range of $\tau_H/\tau_D = 0.16 - 0.18$ and $\tau_H/\tau_{NC} = 8.0 - 8.5$, for $\tau_D/\tau_{FC} = 5.0$ and $\tau_H/\tau_R = 0$, to exhibit cyclic behaviour of the temperature and flow fields. With the new, corrected geometry, this range changes to $\tau_H/\tau_D = 0.16 - 0.20$ and $\tau_H/\tau_{NC} = 8.5 - 14.0$ for $\tau_D/\tau_{FC} = 5.0$ and $\tau_H/\tau_R = 0$. Interestingly, a small change in the geometry and only 5% in volume is enough to change considerably the region for which sustained oscillations in temperature and flow occur for a system without reactant depletion. Furthermore, some cases of damped oscillations were observed for $\tau_D/\tau_{FC} = 5.0$, as discussed previously, which were not reported by Liu and Cardoso [20].

Figure 15a shows the regime diagram for $\tau_D/\tau_{FC} = 5.0$ without reactant consumption ($\tau_H/\tau_R = 0$), with the region where sustained oscillations in temperature, fuel concentration and flow were observed and the cases for which damped oscillations of these fields occurred. Instead of a few isolated cases displaying sustained oscillations [20], it is observed that this phenomena occurs throughout a delimited region, marked

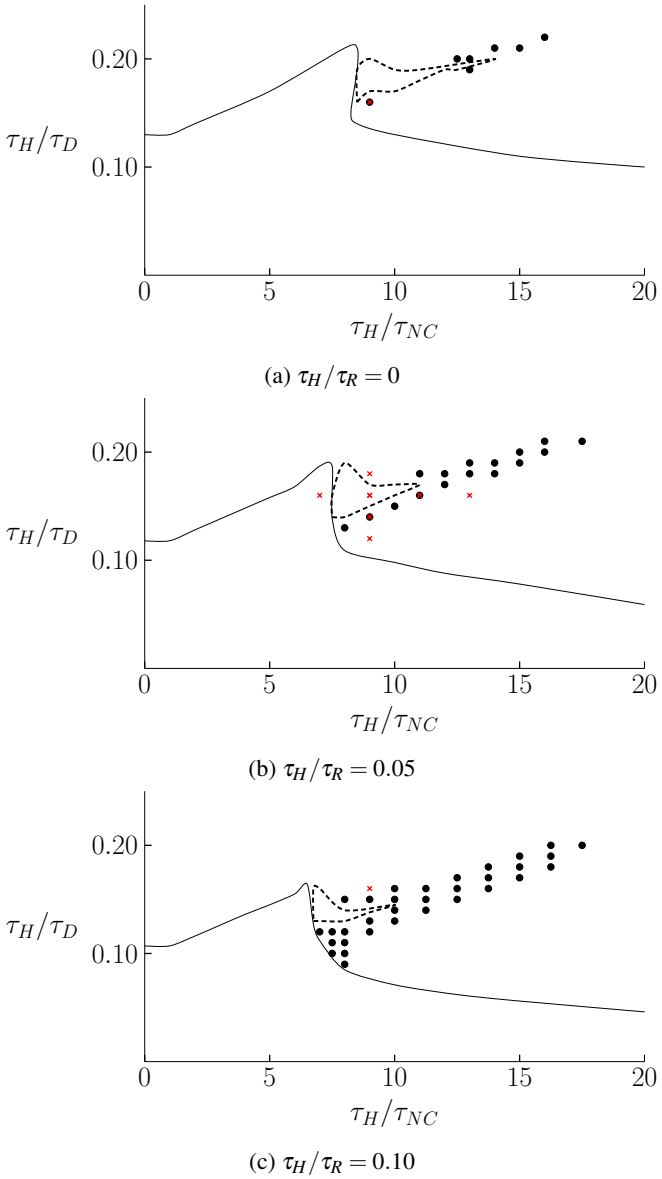

(a) $\tau_H/\tau_R = 0$

(b) $\tau_H/\tau_R = 0.05$

(c) $\tau_H/\tau_R = 0.10$

Fig. 15 Regime diagram for $\tau_D/\tau_{FC} = 5.0$ and different reactant consumption rates showing the explosion boundary (black line), the boundary for sustained oscillations (dashed), and the cases with damped oscillations (dots). The red crosses mark cases I to IX, previously examined.

by the dashed line. The region is larger near the explosion boundary and has an elongated shape pointing diagonally up towards the region of high natural convection and low exothermicity. The cases exhibiting damped oscillations, marked as dots in figs. 15a to 15c for increasing fuel consumption, are positioned in a region which is a protraction of that for the sustained oscillations.

Figure 15b shows the regime diagram and oscillatory region for cases with $\tau_H/\tau_R = 0.05$. It is conspicuous that the range of τ_H/τ_{NC} for which sustained oscillations occur is reduced for these conditions when compared with the systems without reactant consumption of fig. 15a. The oscillatory region is also shifted vertically to lower values of τ_H/τ_D owing to the effects of reactant depletion, but the amplitude of the region and its generic slope in the regime diagram remains nearly unchanged.

The behaviour of the system with stronger fuel consumption ($\tau_H/\tau_R = 0.10$) is depicted in fig. 15c. The range of τ_H/τ_{NC} of the region of sustained oscillations is further reduced and shifted to the left of the diagram when compared to systems with $\tau_H/\tau_R = 0$ and 0.05. Yet, it remains true the amplitude of τ_H/τ_D remains roughly unchanged, even though the reactant consumption effects move the oscillatory region to slightly higher exothermicity values. For strong fuel depletion, cases with damped oscillations in temperature, concentration and fluid flow are observed for a larger region of the regime diagram, not only stretching the tip of the sustained oscillations boundary, as in cases with $\tau_H/\tau_R = 0$ and 0.05, but also connecting it to the explosion boundary below it. By increasing τ_H/τ_D (decreasing exothermicity) for $\tau_H/\tau_{NC} = 8.0$, for example, the system moves from the explosive region to a damped oscillatory behaviour, whereas cases with weak or negligible reactant consumption go through a non-oscillatory region before damped or sustained oscillations occur.

4.2.5 Parametric Conditions for Oscillatory Behaviour

Oscillations occur in a system when there is a "pseudo-balance" of different interacting mechanisms. For the system studied here oscillations in temperature, concentration and flow are attained when the thermal, convective and reactive effects compensate each other cyclically. It is pertinent to investigate under which conditions this balance occurs. Liu and Cardoso [20] predicted that, when the characteristic velocity of natural convection equals that of forced convection, a nearly stagnant region develops in the centre of the vessel, leading to explosion. In the oscillatory cases presented in this work, the hot region is never motionless but undergoes instant stagnation before the buoyant motion overcomes the forced convection. Therefore, a necessary condition for oscillatory behaviour due to balanced convective motion is that the velocity of natural convection is larger than that of forced convection. However, if natural convection dominates, the system will quickly lose heat to the surroundings and reach a steady state without oscillations. Since the main intervenient velocities are the convective ones, it can be assumed that, in order to reach a balance between these two flow forces, the characteristic velocity of natural convection needs to be proportional to the forced convection velocity scale, by a factor α:

$$U_{NC} \sim \alpha U_{FC}. \tag{23}$$

The characteristic velocity for natural convection is

$$U_{NC} \sim (\beta g L \Delta T)^{1/2}, \tag{24}$$

where ΔT is the temperature rise. Since the fluid undergoes instant stagnation, the exothermicity of reaction and heat removal by diffusion are the dominant mechanisms contributing to the temperature rise. Therefore, let ΔT be

$$\Delta T = \frac{q k_0 a_0 L^2}{\kappa \rho_0 C_p}. \tag{25}$$

On the other hand, the forced convection characteristic velocity is approximately

$$U_{FC} \sim u_{ave,i} \frac{L_{i/o}}{L}. \tag{26}$$

Expressing eq. (23) in terms of the governing parameters used in the regime diagrams, one obtains:

$$\frac{\tau_H}{\tau_{NC}} \sim \alpha \frac{L}{L_{i/o}} \frac{\tau_D}{\tau_{FC}} \left(\frac{\tau_H}{\tau_D}\right)^{3/2}. \tag{27}$$

By adjusting the numerical results exhibiting damped oscillations for $\tau_H/\tau_R = 0$ to eq. (27), it is found, through the method of least squares, that a value of $\alpha = 1.5 \pm 0.2$ is a suitable approximation to the results. This means that damped oscillations may take place when the velocity of natural convection is approximately 1.5 times that of forced convection. Since Liu and Cardoso [20] predicted that the peak of the critical τ_H/τ_D value for explosion occurs when these velocities are similar, the sustained oscillatory behaviour is expected for ranges of α between 1.0 and 1.5.

For cases with increasing reactant consumption rates, the damped oscillatory behaviour occurs for slightly lower values of τ_H/τ_D and with a very mild change in the slope of the region when compared with systems without reactant consumption. With less fuel available for reaction, a higher exothermicity is necessary to reach a balance between natural and forced convection, lowering the oscillatory region on the regime diagram. The effect of reactant consumption of a first-order, homogeneous reaction on the critical value of τ_H/τ_D, for sufficiently large values of τ_H/τ_R in closed, diffusive systems, can be described by:

$$\frac{\tau_H}{\tau_D} = \left(\frac{\tau_H}{\tau_D}\right)_{\frac{\tau_H}{\tau_R}=0} \left[1 + \omega \left(\frac{\tau_H}{\tau_R}\right)^{2/3}\right]^{-1}, \tag{28}$$

where ω is a parameter defined as 1.39 by Frank-Kamenetskii [28]. However, Thomas [29] found a value of $\omega = 2.85$, using a different mathematical approach and the Arrhenius approximation, and Gray and Lee [30] later found an inconsistency in the analytical approach made by Frank-Kamenetskii [28], suggesting a corrected value of $\omega = 2.52$. If it is assumed that the change in the damped oscillatory region follows a similar qualitative tendency in terms of dependence on τ_H/τ_R, eq. (27) becomes:

$$\frac{\tau_H}{\tau_{NC}} \sim \alpha \frac{L}{L_{i/o}} \frac{\tau_D}{\tau_{FC}} \left(\frac{\tau_H}{\tau_D}\right)^{3/2}_{\frac{\tau_H}{\tau_R}=0} \left[1 + \omega \left(\frac{\tau_H}{\tau_R}\right)^{2/3}\right]^{-3/2}. \tag{29}$$

Since α is now known for this system, a new value for ω can be sought for cases with both natural and forced convection, by fitting the damped oscillatory cases to eq. (29). Through the method of least squares, a value of $\omega = 0.9 \pm 0.4$ is found to fit the results reasonably well. Figure 16 shows the scaling relation of eq. (29), together with the numerical results, for $\tau_H/\tau_R = 0$, 0.05 and 0.10, and the prediction of Liu and Cardoso [20] for the peaks of the explosion boundary for systems without reactant consumption. The numerical results for the damped oscillatory cases are in good agreement with the parametric predictions discussed here, confirming the previous assumptions of the velocity scales. This also confirms that reactant consumption has an effect on the slope of the oscillatory region in the regime diagram that is qualitatively comparable to that of the reactant consumption effect on the explosion boundary of closed, diffusive systems. Surprisingly, the value of ω is significantly lower than any of the parameters predicted by others [28–30] for the effects of reactant depletion on the explosion boundary. With the introduction of natural and forced convection, one would expect that the magnitude of ω should increase. Nevertheless, the effect of reactant depletion on the balance of natural and forced convection that leads to oscillations is found to be much weaker than the same effect on the explosion boundaries, i.e., the oscillatory behaviour is

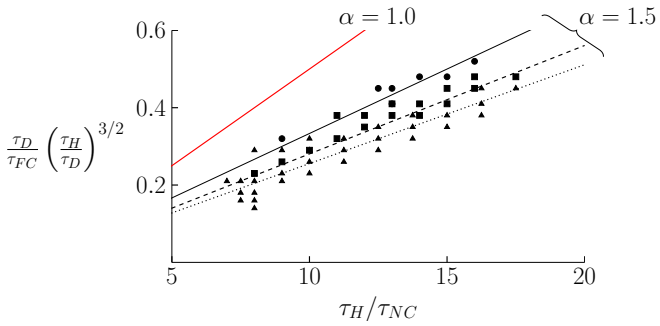

Fig. 16 Parametric conditions for the existence of oscillations in temperature, concentration and flow fields, for cases with $\tau_H/\tau_R = 0$ (circles and solid line), $\tau_H/\tau_R = 0.05$ (squares and dashed line) and $\tau_H/\tau_R = 0.10$ (triangles and dotted line). The black lines represent the scaling condition of eq. (29) ($\alpha = 1.5$) and the red line is the prediction of Liu and Cardoso [20] for the conditions of the peak of the explosion boundary for $\tau_H/\tau_R = 0$ ($\alpha = 1.0$).

more resilient to kinetic effects than explosion. The fact that the oscillations occur in a region of lower exothermicity than that of the explosion boundary can justify this difference: with lower temperature attained in the vessel, the effect of fuel consumption is not as pronounced as in systems reaching higher temperatures, as discussed in section 4.1.

5 Conclusions

The effects of reactant consumption on thermal combustion ($A \rightarrow B$) in a spherical reactor, with both natural and forced convection, have been examined in this work, through numerical simulations. The thermal, convective and kinetic effects were taken into account and quantified by timescales. Two-dimensional regime diagrams were presented for several forced convection intensities (τ_D/τ_{FC}) and reaction consumption rates (τ_H/τ_R), where each axis represented the ratio of timescales for heating-up by reaction and diffusion (τ_H/τ_D) and the ratio of timescales for heating-up by reaction and natural convection (τ_H/τ_{NC}). These regime diagrams delimit not only the explosive region for each system but also the regions where temperature, fuel concentration and flow exhibit sustained or damped oscillations. It was observed that reactant depletion has a stabilising effect on the system, regardless of the natural and forced convection intensities.

The oscillatory behaviour of temperature, reactant concentration and flow fields for systems with moderate forced convection was investigated and a new, unreported phenomena of damped oscillations was analysed in more detail. It was found that reactant consumption has a negligible impact on the range of thermal effects for which sustained oscillations occur but reduces the range of natural convection intensities of the oscillatory region. On the other hand, damped oscillations occur for a larger region of the regime diagram for cases with more fuel depletion than for cases without reactant consumption. A prediction of the parametric conditions for oscillatory behaviour was successfully attained, by extending the expression developed by Frank-Kamenetskii for the effect of reactant consumption on the criticality in closed, diffusive systems to include the effects of both natural and forced convection.

The results presented here provide further understanding of the behaviour of thermal combustion in open systems, showing the regime transitions in terms of relevant physico-chemical parameters.

References

1 N. N. Semenov, *Zeitschrift für Physik*, 1928, **48**, 571–582.
2 D. A. Frank-Kamenetskii, *Diffusion and heat transfer in chemical kinetics*, Plenum Press, 1969, p. 574.
3 A. G. Merzhanov and E. A. Shtessel, *Astronautica Acta*, 1973, **18**, 191–199.
4 A. I. Osipov, A. V. Uvarov and N. A. Roschina, *International Journal of Heat and Mass Transfer*, 2007, **50**, 5226–5231.
5 A. Lazarovici, V. Volpert and J. H. Merkin, *European Journal of Mechanics B-Fluids*, 2005, **24**, 189–203.
6 T. Y. Liu, A. N. Campbell, S. S. S. Cardoso and A. N. Hayhurst, *Physical Chemistry Chemical Physics*, 2008, **10**, 5521–5530.
7 T. Y. Liu, A. N. Campbell, A. N. Hayhurst and S. S. S. Cardoso, *Combustion and Flame*, 2010, **157**, 230–239.
8 D. West, Symposium 'Frontiers in chemical reaction engineering', 2013.
9 K. L. Wasewar, *Chemical and Biochemical Engineering Quarterly*, 2006, **20**, 31–46.
10 E. A. Fox and V. E. Gex, *AIChE Journal*, 1956, **2**, 539–544.
11 A. G. C. Lane and P. Rice, *Industrial & Engineering Chemistry Process Design and Development*, 1982, **21**, 650–653.
12 P. G. Lignola and E. Reverchon, *Combustion Science and Technology*, 1988, **60**, 319–333.
13 D. Matras and J. Villermaux, *Chemical Engineering Science*, 1973, **28**, 129–137.
14 P. Dagaut, M. Cathonnet, J. P. Rouan, R. Foulatier, A. Quilgars, J. C. Boettner, F. Gaillard and H. James, *Journal of Physics E: Scientific Instruments*, 1986, **19**, 207.
15 P. Dagaut, *Physical Chemistry Chemical Physics*, 2002, **4**, 2079–2094.
16 N. Leplat, P. Dagaut, C. Togbé and J. Vandooren, *Combustion and Flame*, 2011, **158**, 705–725.
17 J. D. Jackson, M. A. Cotton and B. P. Axcell, *International Journal of Heat and Fluid Flow*, 1989, **10**, 2–15.
18 F. Santarelli and F. P. Foraboschi, *The Chemical Engineering Journal*, 1973, **6**, 59–68.
19 E. Arquis, O. Amiel, R. Salmon, N. Richard and J. P. Caltagirone, *Journal of Heat Transfer*, 1993, **115**, 1066–1069.
20 T. Y. Liu and S. S. S. Cardoso, *Combustion and Flame*, 2013, **160**, 191–203.
21 J. S. Turner, *Buoyancy effects in fluids*, Cambridge University Press, Cambridge, 1979.
22 D. D. Gray and A. Giorgini, *International Journal of Heat and Mass Transfer*, 1976, **19**, 545–551.
23 CSIRO, *Fastflo Tutorial Guide (version 3)*, 1998.
24 F. Gonçalves de Azevedo, J. F. Griffiths and S. S. S. Cardoso, *Physical Chemistry Chemical Physics*, 2013, **15**, 16713–16724.
25 A. N. Campbell, S. S. S. Cardoso and A. N. Hayhurst, *Combustion and Flame*, 2008, **154**, 122–142.
26 S. S. S. Cardoso, P. C. Kan, K. K. Savjani, A. N. Hayhurst and J. F. Griffiths, *Physical Chemistry Chemical Physics*, 2004, **6**, 1687–1696.
27 W. H. Archer, *PhD thesis*, Institute of Science and Technology, University of Manchester, 1977.
28 D. A. Frank-Kamenetskii, *Diffusion and heat transfer in chemical kinetics*, Princeton University Press, Princeton, 1955, p. 370.
29 P. H. Thomas, *Proceedings of the Royal Society of London Series A - Mathematical and Physical Sciences*, 1961, **262**, 192–206.
30 P. Gray and P. R. Lee, *Combustion and Flame*, 1965, **9**, 201–203.

Thermal explosion and oscillatory behaviour in the presence of coupled forced and natural convection in a spherical reactor.